ACS APPLIED MATERIALS & INTERFACES

Research Article

www.acsami.org

Synthesis and Properties of a Novel Structural Binder Utilizing the Chemistry of Iron Carbonation

Sumanta Das,[†] Beshoy Souliman,[‡] David Stone,[∥] and Narayanan Neithalath*[,§]

[†]School of Sustainable Engineering and the Built Environment, [‡]School of Sustainable Engineering and the Built Environment, and [§]School of Sustainable Engineering and the Built EnvironmentArizona State University, Tempe, Arizona 85004, United States

[∥]Iron Shell LLC, Tucson, Arizona 85717, United States

Supporting Information

ABSTRACT: This paper explores, for the first time, the possibility of carbonating waste metallic iron powder to develop sustainable binder systems for concrete. The fundamental premise of this work is that metallic iron will react with aqueous CO_2 under controlled conditions to form complex iron carbonates which have binding capabilities. Chosen additives containing silica and alumina are added to facilitate iron dissolution and to obtain beneficial rheological and later-age properties. Water is generally only a medium for mass transfer in these systems thereby making the common reaction schemes in portland cement concretes inapplicable. The compressive and flexural strengths of the chosen iron-based binder systems increase with carbonation duration and the specimens carbonated for 4 days exhibit mechanical properties that are comparable to those of companion ordinary portland cement systems that are most commonly used as the binder in building and infrastructural construction. The influence of the additives, carbonation duration, and the air curing duration after carbonation are explored in detail. Thermogravimetric analysis demonstrate the presence of an organic carbonate complex (the dissolution agent used to dissolve iron is organic), the amount of which increases with carbonation duration. Thermal analysis also confirms the participation of some amount of limestone powder in the reaction product formation. The viability of this binder type for concrete applications is proved in this study.

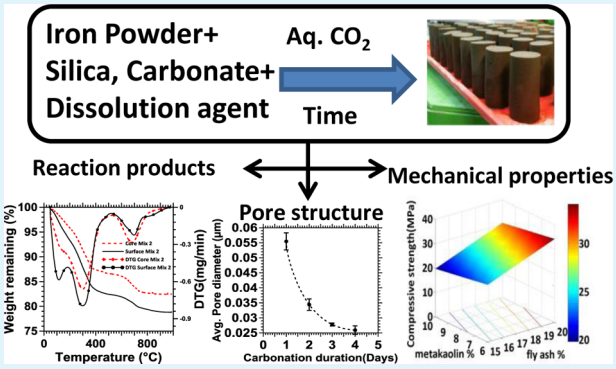

KEYWORDS: *iron powder, sustainable binder, carbonation, compressive strength, pore size, thermogravimetric analysis*

1. INTRODUCTION

Methods to reduce the amount of greenhouse gases (GHG), such as CO_2 in the atmosphere is an active research area.[1−7] Mineral route of carbonation, where mined mineral rocks are used as the feedstock through which CO_2 is passed is one of the promising routes to reduce the concentration of CO_2 in the atmosphere.[8−10] One of the major benefits of mineral carbonation is that CO_2 is chemically sequestered (as opposed to physical sequestration in almost all other methods, which is not always leakage-proof), thus making the sequestration virtually permanent. It has also been noticed that the secondary carbonate rocks formed during mineral trapping demonstrate mechanical strength[11−13] which opens up the possibility of using of mineral trapping in conjunction with sustainable binder production for construction. Magnesium oxide bearing rocks such as olivine and serpentine have been used as candidates for mineral carbonation; however, possibilities exist for the use of several other metal or alkali metal species to be beneficially carbonated.[14−16]

In this paper, the results of a material design study that investigates the potential of formation of a novel binder from metallic waste iron powder is reported. [The study reported here outlines for the first time, the general idea toward the development of this novel material. Several follow-up studies on mechanical, rheological, and durability studies are necessary to ensure widespread practical acceptance. This study is the first step in that direction.] Metallic iron powder is generated in significant amounts as bag-house dust waste during the electric arc furnace (EAF) manufacturing process of steel and from the shot-blasting operations of structural steel sections. The traditional means of disposing EAF and shot-blasting dust is landfilling as it is not economically feasible to recycle the iron from the dust. Several million tons of such waste material is being landfilled at great costs all over the world. In the present work, an approach to form a sustainable binder system for concretes from carbonation of iron dust is proposed, which is inspired by the idea of CO_2-corrosion of, and scale formation in carbon-steel pipelines in the oil and gas industry, which is a result of CO_2 injection into the oil wells to reduce the viscosity of the oil and thus increase oil production.[17] The novel binder system, relying on the beneficial effects of "corrosion" of iron particles to form a binding matrix provides yet-unheard-of

Received: February 24, 2014
Accepted: May 19, 2014
Published: May 19, 2014

   dx.doi.org/10.1021/am5011145 | ACS Appl. Mater. Interfaces 2014, 6, 8295−8304

synergistic benefits through: (i) consumption and trapping of CO_2 from a GHG-emitting industrial operation and subsequent carbonate formation, and (ii) providing a means to reduce the overall Ordinary Portland Cement (OPC) production (which is a significant emitter of GHG) through the use of carbonated metallic iron powder as the binder material for concrete.

Several studies on iron carbonate formation by CO_2 corrosion of steel have been reported.[18−20] The most common reaction of iron involves the formation of oxides. However, dissolved CO_2 is also capable of reacting with iron where a dense layer of iron carbonate forms and adheres strongly to the substrate. The accepted reaction steps for this process are[21]

$$Fe + 2CO_2 + 2H_2O \rightarrow Fe^{2+} + 2HCO_3^- + H_2\uparrow \quad (1)$$

$$Fe^{2+} + 2HCO_3^- \rightarrow FeCO_3 + CO_2 + H_2O \quad (2)$$

The net reaction then is

$$Fe + CO_2 + H_2O \rightarrow FeCO_3 + H_2\uparrow \quad (3)$$

Though the basic reaction scheme seems straightforward and simplistic, the kinetics of the reaction and the rate of product formation are often very slow so as to be of any use for beneficial industrial applications. Hence dissolution agents (organic) that have the potential to enhance the corrosion rate of iron due to their high reducing power and complexing capacity[22−24] need to be employed to control the reaction rates. In addition, several other factors are important when an alternate material is being considered for applications that commonly use Portland cement. These relate to early age properties including the rheological behavior (flowability and castability) and early strength development. Hence additives common to portland cement concretes such as class F fly ash, powdered limestone, and metakaolin have been used in this study as minor ingredients along with metallic iron powder to form pastes with adequate binding capabilities. Fly ash has been added as a source of silica to potentially facilitate iron silicate complexation,[25,26] whereas fine limestone powder provides additional nucleation sites, and metakaolin provides cohesiveness in the fresh state to the iron-based mixtures. This paper reports the proportions of iron powder and other additives, and investigates the influence of curing regime (CO_2 and air-exposure) for desired mechanical properties of these binder systems. Characterization of the reaction products in these binder systems is carried out using thermogravimetric analysis in this paper. A proper understanding of the influence of source materials and processing on the mechanical properties of this unique binding system is expected to contribute to other related studies on this sustainable material as well as lead to entrepreneurial ventures to make beneficial products out of this technology, which is the ultimate objective of this research task.

2. EXPERIMENTAL PROGRAM

2.1. Starting Materials: Composition and Particle Size. Metallic iron powder with median particle size of 19 μm is used as the main starting material in this study. The iron powder is obtained from a shot-blasting facility in Phoenix, AZ. The iron powder has mostly elongated and plate-like particles as can be seen from the electron micrograph shown in Figure 1, thereby influencing the rheological properties of the mixture. However, the larger surface area-to-volume ratio of this shape as compared to the spherical shape provides benefits related to reactivity. The iron powder consists of 88% Fe and 10% O (some amount of atmospheric oxidation) along with trace quantities of Cu, Mn, and Ca.

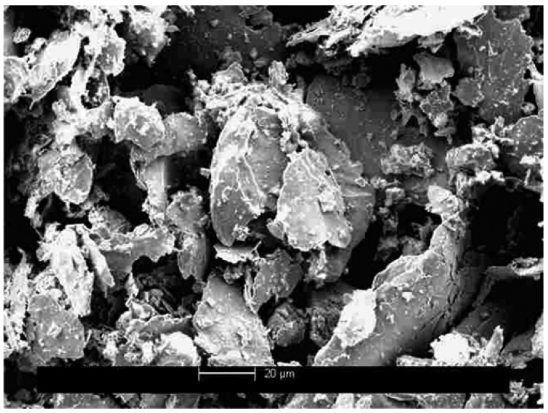

Figure 1. Scanning electron micrograph of iron particles. The scale bar corresponds to 20 μm.

The other materials used in the binder include Class F fly ash and metakaolin conforming to ASTM C 618, and limestone powder with a median particle size 0.7 μm conforming to ASTM C 568. Fly ash was used to provide a silica source for the reactions (to potentially facility iron silicate complexation),[25,26] fine limestone powder to provide nucleation sites, and metakaolin to provide cohesiveness in the fresh state to the iron-based mixtures. [Other more reactive silica sources, such as silica fume, can also be used, but fly ash has been chosen partly to make beneficial use of its spherical shape that enhances the workability characteristics of the suspension.] It needs to be remembered that the water is reduced in the chemical reactions but does not form part of the binder. Hence, to minimize the water demand, yet keeping the consistency and cohesiveness of the mixture, metakaolin was used. An organic reducing agent/chelating agent for metal cations was also used. Commercially available type I/II ordinary Portland cement (OPC) conforming to ASTM C 150 was used to prepare conventional cement pastes and compare the compressive strengths of the novel iron-based binder systems with those of the traditional OPC-based systems. OPC was also partially replaced by class F fly ash and blast furnace slag up to 40% and 50% respectively by mass for comparison purposes. Fly ash contains about 60% by mass of SiO_2 whereas the siliceous content of metakaolin is about 50%. The limestone powder used is a nominally pure calcium carbonate (97% by mass).

The particle size distributions of the iron powder, fly ash, metakaolin, limestone powder and OPC, obtained from a laser diffraction-based particle size analyzer are shown in Figure 2. All the ingredients are finer than the iron powder used. Please note that the quantified data presented in this paper could vary based on iron powder fineness, but the general mechanisms and trends are expected to remain the same. [Note that reducing the fineness does not always result in strength enhancement for the iron carbonate binders contrary to the observations for OPC mixtures. Larger size iron particles with a smaller carbonation ring that is just sufficient to facilitate the binding of adjacent particles could result in better properties (flexural and fracture response in particular) because of the superior properties of the iron core.]

2.2. Mixing Procedure and Sample Preparation. The mixing procedure involves initial dry mixing of all materials (iron powder, fly ash, limestone powder, metakaolin, and the organic reducing agent). Water was then added and mixed to obtain a uniform cohesive mixture. The mass-based water-to-solids ratio (w/s) was varied between 0.22 and 0.25 depending upon the proportions of the constituents in the mixtures to attain a cohesive mix. Since the carbonation process of iron does not incorporate water in the reaction products and it is merely an agent of mass-transfer, the w/s used is primarily based on the criteria of obtaining desired workability, castability, and ability to strip the molds without specimen breakage. The mixture was then tamped into cylindrical molds (32.5 mm diameter × 65 mm long) of the Harvard miniature compaction

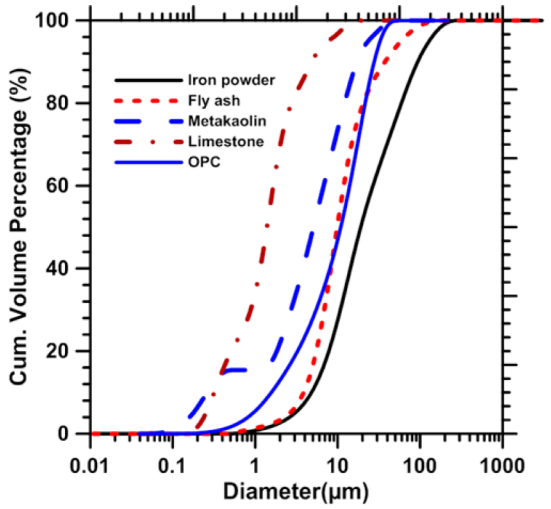

Figure 2. Particle size distribution of metallic iron powder, OPC, fly ash, metakaolin, and limestone powder.

apparatus (ASTM D 4609, Annex A1) in five layers to fill the mold completely. The specimens were demolded immediately using a specimen ejector for the compaction apparatus and placed inside clear plastic bags filled with 100% CO_2 in room temperature inside a fume hood for 1 to 4 days. The bags were refilled with CO_2 every 12 h so as to maintain saturation inside the chamber. After the respective durations of CO_2 exposure, the samples were placed in air at room temperature to allow the moisture to evaporate for 1 to 30 days. The OPC-based systems for comparative evaluations were cast in 50 mm cube molds and moist-cured (>98% RH and 23 ± 2 °C) for 7 days before compressive strength testing. The water-to-cementitious materials ratio (w/cm) adopted for the OPC-based mixtures was 0.40, which is the most common w/cm used for moderate strength (20−35 MPa) concretes.

2.3. Determination of Desirable Mixture Proportions and Curing Procedure. A total of eight different mixtures with varying iron powder, fly ash, limestone, and metakaolin contents were proportioned in this preliminary study to select a few best performing mixtures, first in terms of compressive strength. The iron powder content ranged from 58% to 69% by mass. The fly ash content was maintained at 15% or 20%, limestone content at 8% or 10%, and metakaolin content at 6% or 10%. The w/s ratios varied between 0.22 and 0.25. These preliminary proportions were arrived at based on several trial proportions that used iron powder from 50% to 100% of the total binder content along with the other ingredients at multiple levels beyond the ranges described above, and several w/s ratios in the range of 0.15 to 0.30. The proportions of the eight short-listed mixtures are shown in Table 1. These proportions were chosen such

Table 1. Proportions of the Mixtures Chosen in This Study

	contents (% by mass of the total powder) of the different ingredients in mixture							
component materials	1	2	3	4	5	6	7	8
iron powder	64	60	62	58	69	65	67	63
fly ash	20	20	20	20	15	15	15	15
limestone	8	8	10	10	8	8	10	10
metakaolin	6	10	6	10	6	10	6	10

that they were able to be compacted into molds to create a homogeneous mixture and able to be demolded without breakage. In all cases, the organic reducing agent, which is a weak acid (oxalic acid in this case),[22−24] was added in a powder form at 2% of total mass of the constituents. This was arrived at based on the solubility of the organic acid in water, and the fact that at this dosage, the resultant mixtures exhibited almost double the compressive strength as the mixtures without the dissociating agent. More studies on optimizing the dosage of the dissociation agent are needed.

For the preliminary study, the specimens were kept in a 100% CO_2 atmosphere for 3 days immediately after casting and demolding, and cured in air for 2 days before they were tested in uniaxial compression. The best performing mixture contained 60% iron powder, 20% fly ash, 8% limestone, and 10% metakaolin (mixture number 2 in Table 1) whereas another mixture containing 64% iron powder, 20% fly ash, 8% limestone, and 6% metakaolin (mixture number 1 in Table 1) also performed quite similarly in terms of average compressive strength (>25 MPa). Once the two best performing mixtures were determined, the CO_2 curing duration was varied from 1 to 4 days and the air curing duration varied from 1 to 3 days to determine the optimal combination of CO_2 and air-curing durations from among these conditions. The upper limit of the carbonation duration was chosen based on the thermogravimetric analysis (TGA) results (presented later) which showed similar degrees of carbonation in the core and surface of the cylindrical samples after 4 days of carbonation. Air-curing was extended to 30 days, but no appreciable changes in compressive strengths were found after 3 days.

Flexural strength tests were also carried out on two best performing mixtures under compression. Paste beams, 250 mm × 25 mm × 25 mm in size were prepared and cured in a 100% CO_2 environment for 2−6 days. The air-exposure time was maintained constant at 3 days. Three-point bending tests were conducted at a displacement rate of 0.375 mm/min until the samples failed.

2.4. Thermogravimetric Analysis (TGA). A PerkinElmer STA 6000 simultaneous thermal analyzer was used for thermogravimetric analysis (TGA). The analyzer was programmed to increase the temperature from 30 to 995 °C at a rate of 15 °C/min in a N_2 environment. The samples for TGA were obtained from the cylindrical samples that were cured for the compressive strength tests. Samples from both surface as well as core of the cylindrical specimens were analyzed in order to assess the influence of CO_2 penetration on the degree of reaction.

2.5. Mercury Intrusion Porosimetry (MIP). Mercury intrusion porosimetry (MIP), which is a well-established technique to investigate the pore structure of porous materials, was adopted to study the pore structure. The samples for MIP tests were taken from the core of the cylindrical sample. The MIP test was done in two steps: (i) evacuation of gases, filling the sample holder with mercury, and increasing the pressure up to 345 kPa, and (ii) intrusion of the mercury into the sample at high pressures (up to 414 MPa). The contact angle and surface tension of Hg used for the analysis was 0.485 N/m. In the absence of a better understanding of the contact angle between Hg and the iron carbonate binder, the common value used for OPC-based pastes (130°) was used here. The comparative nature of the evaluations attempted here justify the use of this approximate value. The pore diameters were evaluated using the Washburn equation,[29−31] based on the assumption that the pores are of cylindrical shape. A minimum pore diameter of 0.003 μm can be evaluated using MIP. The average pore diameter (d_a) can be estimated[28] for varying carbonation durations using the total volume of mercury intruded (V, cm^3/g) and the pore surface area (A, cm^2/g) obtained from MIP as

$$d_a = (4V/A) \quad (4)$$

3. RESULTS AND DISCUSSION

3.1. Influence of Source Materials and Curing Conditions on Compressive Strength. *3.1.1. Influence of Source Materials and Determination of Optimal Mixtures for Compressive Strength.* As mentioned earlier, eight different mixtures (Table 1) were proportioned to understand the effects of various constituents on compressive strength of iron carbonate binders and to determine the optimal mixtures in terms of compressive strength for a specific curing duration and procedure. The samples were kept in a CO_2 environment for 3

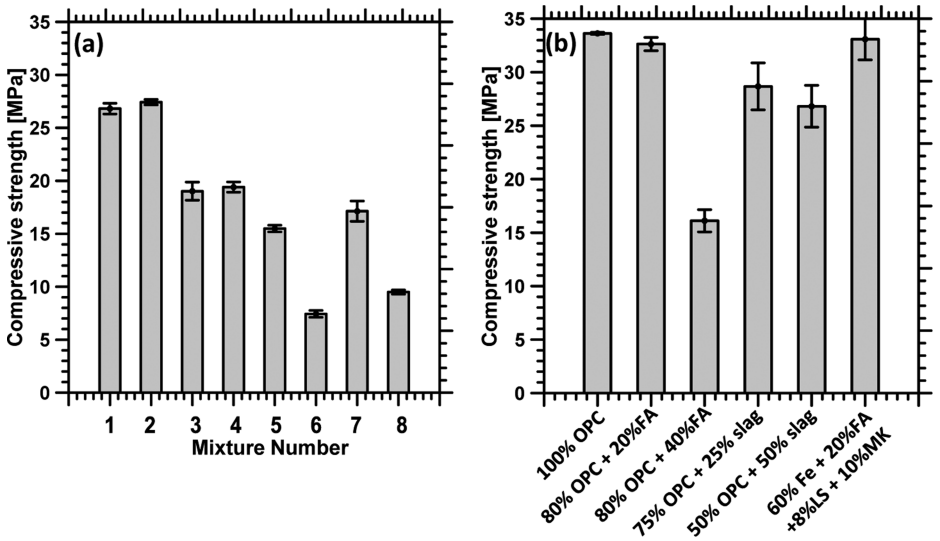

Figure 3. (a) Compressive strength values of the mixtures (3 days in CO_2 and 2 days in air) and (b) 7-day compressive strengths of plain and modified OPC mixtures for comparison with 4-day carbonated iron−carbonate (mixture 2 60% iron powder, 20% fly ash, 8% limestone, 10% metakaolin).

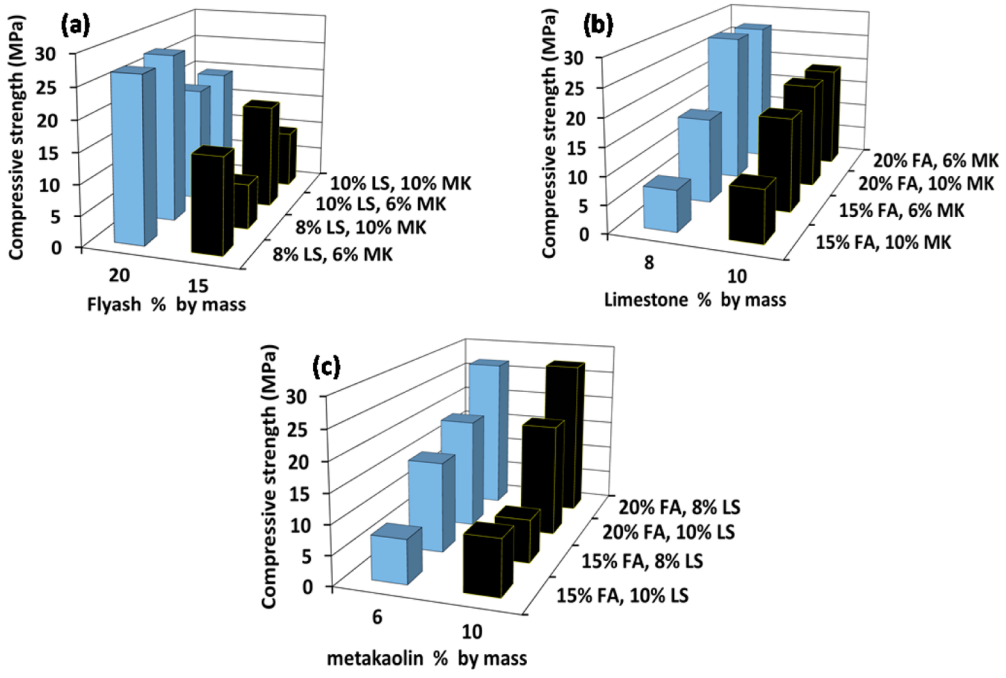

Figure 4. Effect of (a) fly ash, (b) limestone, and (c) metakaolin contents on compressive strength of iron carbonate binders.

days and then cured in air for 2 days at 23 ± 2 °C to get a comparative idea of the compressive strengths of these eight mixtures. The compressive strengths of different mixtures are reported in Figure 3a, from which it can be observed that Mixtures 1 and 2 are the best performing ones. The variability of strength between a number of identical samples tested is also low as can be observed from this figure. Figure 3b shows the 7-day compressive strengths of moist-cured OPC-based pastes with and without several cement replacement materials for comparison, which demonstrates the similarity in strengths at the chosen ages of treatment. While it is well-known that OPC-based systems gain strength over a period of time due to continued cement hydration and will likely end up with higher compressive strengths, the values reported here for iron carbonate-based binder systems are in the range of strengths that can be used for a large number of construction applications.

The influence of various constituents on compressive strength is elaborated in Figure 4. Figure 4(a) implies that the samples with 20% fly ash were significantly stronger than the ones with 15% fly ash, irrespective of the contents of limestone and metakaolin. Both the best performing mixtures (mixture 1 and 2) contained 20% fly ash by mass. These mixtures also demonstrated the lowest porosity, as determined from mercury intrusion porosimetry, plausibly because of the combined effect of particle packing and increased reaction product formation (as will be confirmed from TGA results in a later section). From Figure 4(b), it can be seen that the limestone content exerts negligible influence on compressive strength at lower fly ash contents, but at higher fly ash contents,

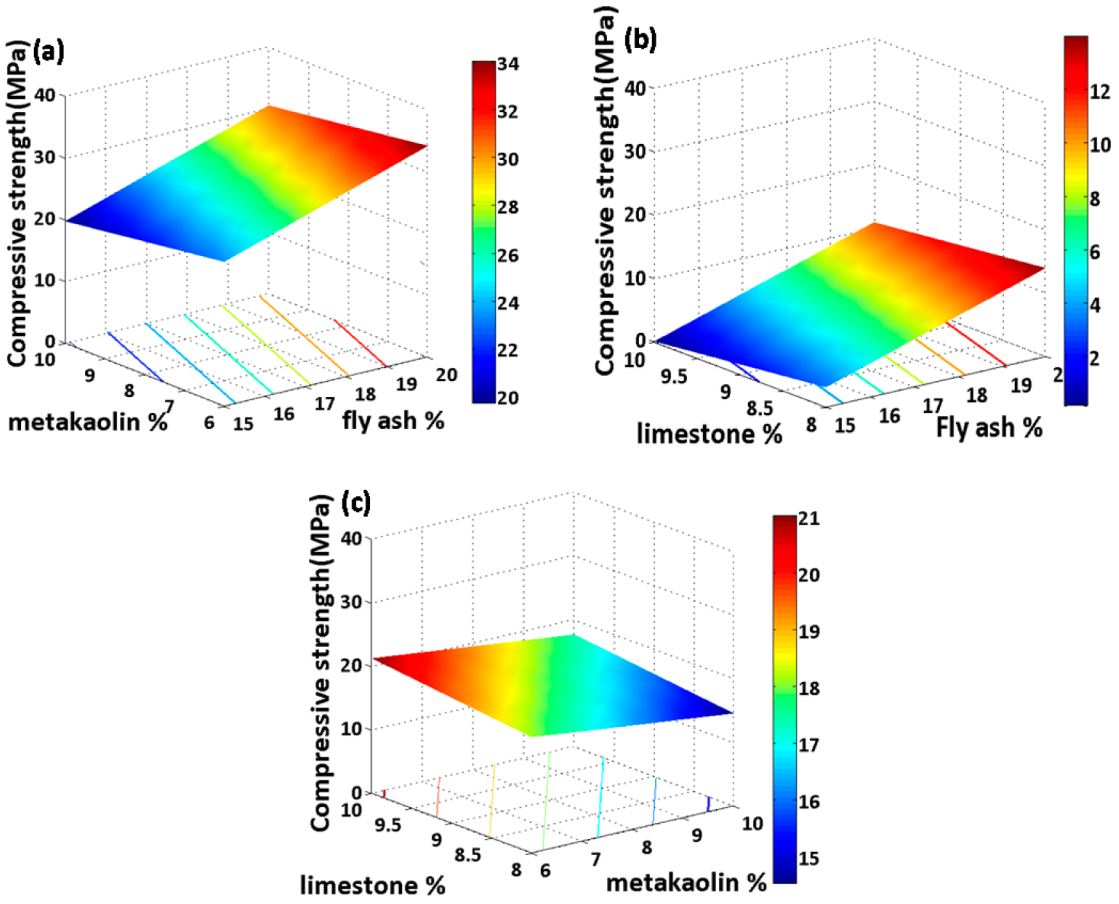

Figure 5. Response surfaces showing the statistical influence of amounts of (a) fly ash and metakaolin, (b) fly ash and limestone, (c) metakaolin and limestone, on compressive strength.

a lower amount of limestone powder is preferable. Compressive strength is relatively insensitive to variations in metakaolin content for the samples containing 20% fly ash as the synergistic effect of silicates and cohesive nature of metakaolin likely ensures a denser matrix. At a lower fly ash content, an increase in the metakaolin content is associated with significant decrease in the compressive strength values, attributable to the increased water retention by metakaolin (since it is of clayey origin) and the lack of enough amounts of fly ash to enhance the workability and produce a consistent and defect-free mixture.

To discern the statistical influence of the amounts of fly ash, metakaolin, and limestone on the compressive strength and the relative sensitivity of strength to these factors, a 2^3 factorial analysis was carried out. The response surfaces of compressive strength are shown in Figure 5. It is confirmed that fly ash is the dominant factor among the three as far as compressive strength is concerned. The sensitivity of compressive strength to variations in the amount of limestone and metakaolin is relatively low. Metakaolin is basically used as a rheology modifier in these systems whereas the fine limestone is expected to be a nucleation site for the reaction products. The range of amount of limestone used in this study (8−10%) does not significantly impact the strength. More studies are required to understand how fine limestone powder participates in the reactions; however, TGA studies in the forthcoming section do indicate some consumption of limestone in the reaction to form a carbonate-containing complex reaction product.

As discussed earlier, Figure 3a does not provide any realistic differences in strengths between mixtures 1 and 2 under the chosen curing condition (in a CO_2 environment for 3 days and air-cured for 2 days). To observe whether changes in curing conditions would elicit varied response from these mixes, the cylindrical specimens were carbonated for 3 or 4 days and air-cured for 1 or 3 days. Figure 6 demonstrates the strengths of these mixes after being cured under such conditions. Here the

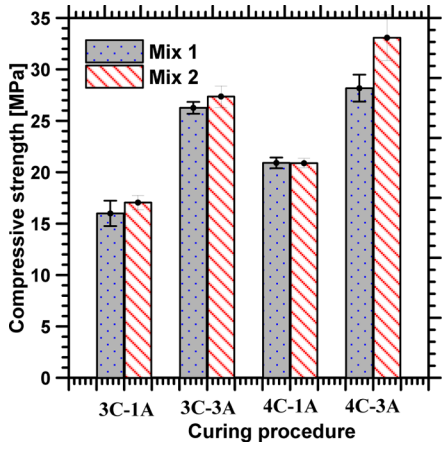

Figure 6. Comparison of compressive strength of mixtures 1 (64% iron powder, 20% fly ash, 8% limestone, 6% metakaolin) and 2 (60% iron powder, 20% fly ash, 8% limestone, 10% metakaolin) under different curing conditions.

dx.doi.org/10.1021/am5011145 | ACS Appl. Mater. Interfaces 2014, 6, 8295−8304

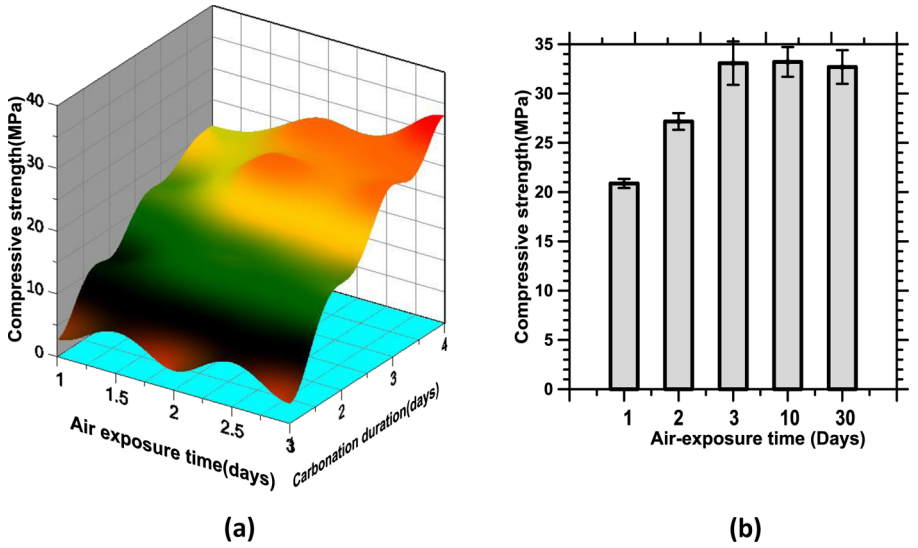

Figure 7. Effect of (a) curing procedure and curing duration. (b) Air-curing duration on compressive strength of mixture 2 (60% iron powder, 20% fly ash, 8% limestone, 10% metakaolin). The samples were carbonated for 4 days for the data in panel b.

number before "C" represents the days of carbonation, whereas the number before "A" represents the air-exposure time in days. Mixture 2 was chosen for all further studies reported here because it performed similar to or better than mixture 1 for all the curing regimes in terms of compressive strength as can be observed from Figure 6.

3.1.2. Effect of Curing Conditions on Compressive and Flexural Strengths. The effects of curing procedure and duration on compressive strengths of the iron carbonate binders are shown in Figure 7. The samples were cured in CO_2 for 1 to 4 days and in air for 1 to 3 days thereafter. The strength values are shown in a response surface plot as a function of CO_2 and air-curing durations in Figure 7a. The influence of CO_2 curing duration is obvious from this figure. The compressive strength values were very low for the samples cured in CO_2 for 1 day only due to the very low degree of carbonation. Since it is the carbonation that provides the mechanical strength, there is no discernible strength increase when the moisture leaves the system through air exposure. This can be seen from this figure where for 1 day of carbonation, increasing the air exposure duration from 1 to 3 days does not impact the compressive strength positively. However, the effect of air-curing is evident when the carbonation duration is increased. A significant increase in strength is observed for specimens carbonated for a longer duration when the air curing time was increased. This is attributed to the fact that the average pore sizes decrease with increased carbonation duration as shown in Figure 8, for mixture 2. The average pore size of the 1-day carbonated samples are larger, which consequently exerts less internal moisture pressure under a compression test (pressure is inversely proportional to the pore size) and therefore loss of moisture through air exposure does not have a larger effect on internal pressure and thus the compressive strength. The pore sizes of samples carbonated for a longer duration are lower due to increased reaction product formation, resulting in an increased sensitivity of compressive strength to the loss of moisture. In order to clearly bring out the effect of air exposure, Figure 7b plots the compressive strengths as a function of air exposure duration after the samples were carbonated for 4 days. First 3 days of exposure to air results in an enhancement in the compressive strength but as the moisture dries out completely,

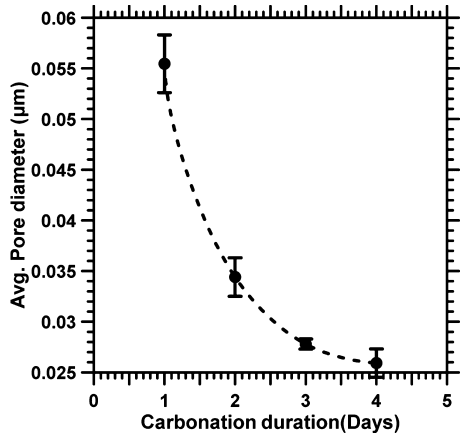

Figure 8. Variations in average pore diameter with varying carbonation durations for mixture 2 (60% iron powder, 20% fly ash, 8% limestone, 10% metakaolin).

there is no significant change in compressive strength which signifies that the reaction product is passive and stable in air and it does not cause any deterioration when exposed to air for longer time periods. Thus, the air exposure duration (depending on the pore structure of the material that lets moisture escape from the bulk of the specimen) influences the compressive strength at longer carbonation durations.

Figure 9a shows the variation in flexural strength of iron carbonate binders (both mixtures 1 and 2) with an increase in carbonation duration. The flexural strengths are very similar for both the mixtures, which is in line with the trends for compressive strength. It can be noticed that a carbonation duration of 6 days result in a relatively high flexural strength of about 8 MPa. In comparison, general OPC-based systems demonstrate a flexural strength of 3−4 MPa. This increased flexural strength makes this binder an interesting option for several applications that rely on improved flexural properties (beams, pavement slabs, etc.) Figure 9b shows the relationship between flexural strength and density for these mixes. Higher carbonation durations results in more reaction product formation and increased density as the reaction product fills the pores more efficiently.

dx.doi.org/10.1021/am5011145 | ACS Appl. Mater. Interfaces 2014, 6, 8295−8304

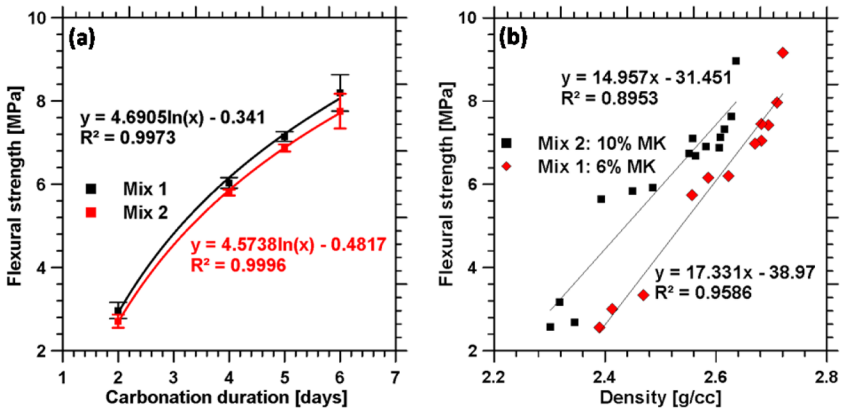

Figure 9. (a) Logarithmic increase of flexural strength with increase in carbonation duration and (b) interaction between bulk density and flexural strength. Mixture 1 (64% iron powder, 20% fly ash, 8% limestone, 6% metakaolin) and mixture 2 (60% iron powder, 20% fly ash, 8% limestone, 10% metakaolin). Note that the iron-based binder paste is only about 20−25% denser that common portland cement-based pastes. When concretes that contain about 70% aggregates by volume are considered, the density differences drops down to about 10%.

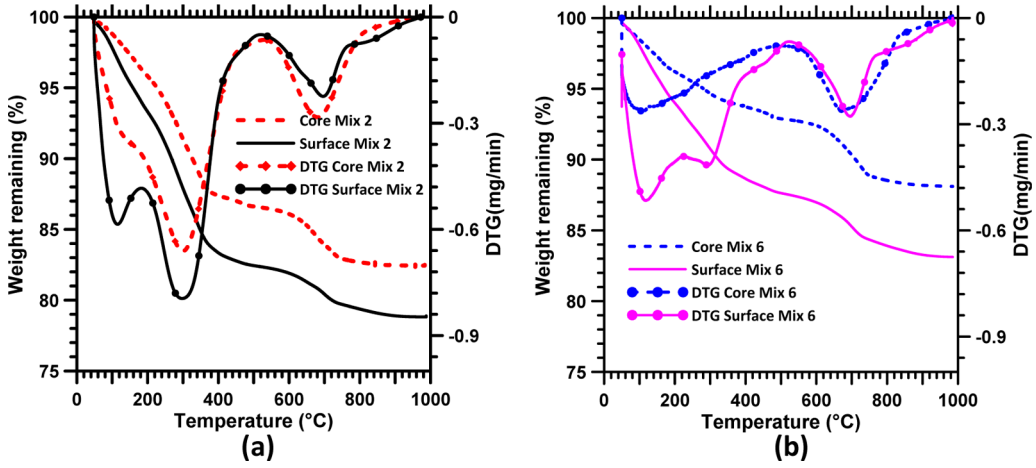

Figure 10. TG and DTG curves corresponding to the core and surface of: (a) Mixture 2 (60% iron powder, 20% fly ash, 8% limestone, 10% metakaolin), and (b) Mixture 6 (65% iron powder, 15% fly ash, 8% limestone, 10% metakaolin), carbonated for 3 days.

3.2. REACTION PRODUCTS AND EXTENT OF CARBONATION

Thermogravimetric analysis was carried out on powdered samples extracted from the surface as well as the core of the cylindrical specimens to investigate the degree of reaction that is responsible for differences in mechanical properties. First, thermal analysis results of mixtures 2 and 6 have been compared in order to understand the differences in product constitution between the best and worst performing mixtures as far as compressive strength is concerned. The major differences between these mixtures are in the iron powder and fly ash contents. Figure 10a and b depicts the TG curves and their derivatives for the samples from the surface and core of cylindrical specimens corresponding to these mixtures. Both the specimens were carbonated for 3 days. A comparison of Figure 10a and b suggests that the total weight loss for mixture 2 is significantly higher than that for mixture 6, indicating that the overall degree of reaction and product formation is lower under the chosen carbonating conditions for the starting material combination of mixture 6. The total weight loss of the sample from the surface of mixture 6 cylinder is slightly lower than the weight loss from the core sample of mixture 2 cylinder. This shows that the constitution of mixture 6 is not amenable to desirable levels of carbonation and product formation, which reflects in the compressive strength of the binder. This observation also points to the fact that the carbonation efficiency and mechanical properties of iron carbonate binders are very sensitive to the overall starting material composition—from a compositional viewpoint, the differences between mixtures 2 and 6 are not very large. It should also be considered that the range of iron powder contents that provided reasonable strengths were rather narrow, between 60% and 69%, as shown in Table 1.

The DTG curves demonstrate three distinct peaks for the binder samples as can be observed in Figure 10. The peak at around 110 °C is attributed to evaporable water, the one at around 300 °C to products belonging to the carbonate-oxalate-cancrinite group,[27] and the one at around 740 °C to calcium carbonate. The DTG for mixture 2 provides a strong, distinct peak at about 300 °C (for samples from both the core and the surface) whereas the intensity of the peak reduces for samples from mixture 6. The peak is almost nonexistent for the sample from the core of mixture 6, indicating that the carbonation efficiency for that mixture constitution is low.

Further, the effect of carbonation duration on reaction product formation is investigated and explained using Figure 11. Figure 11 shows the TG and DTG curves for samples of Mixture 2 corresponding to the surface and core of the

dx.doi.org/10.1021/am5011145 | ACS Appl. Mater. Interfaces 2014, 6, 8295−8304

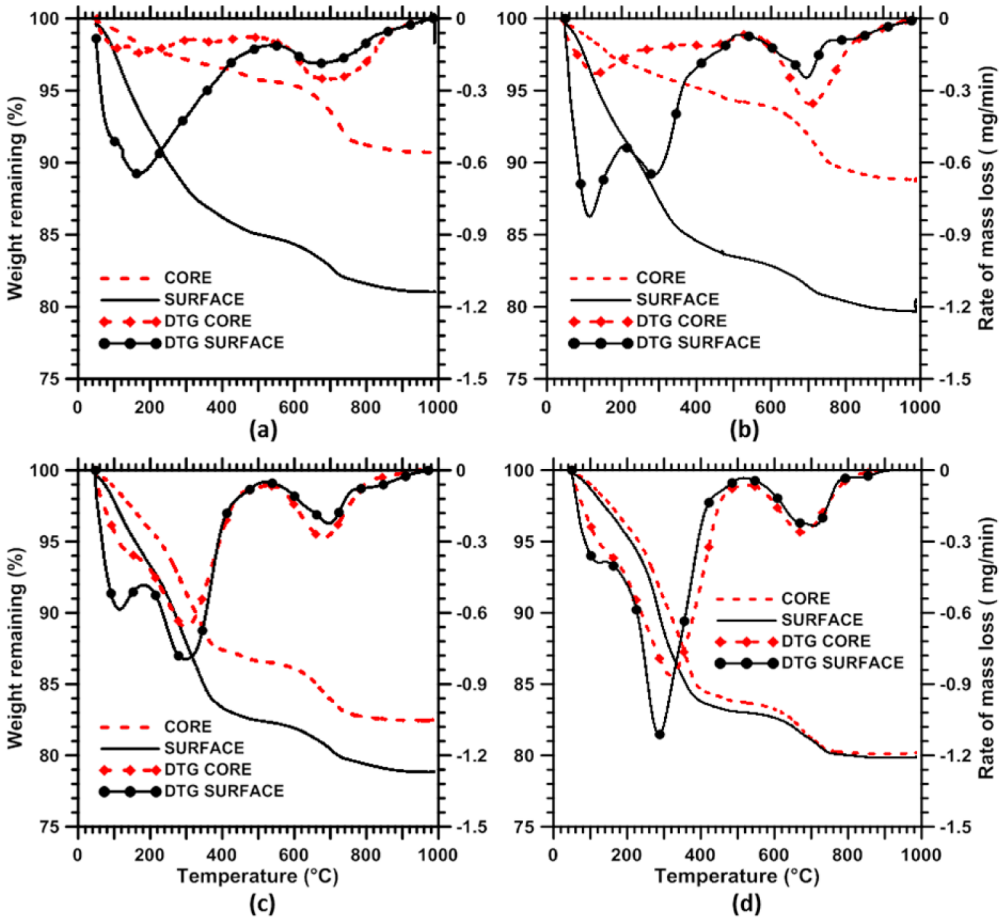

Figure 11. Thermal analysis results of samples from mixture 2 (60% iron powder, 20% fly ash, 8% limestone, 10% metakaolin) carbonated for (a) 1, (b) 2, (c) 3, and (d) 4 days. All samples were exposed to air for 3 days after carbonation.

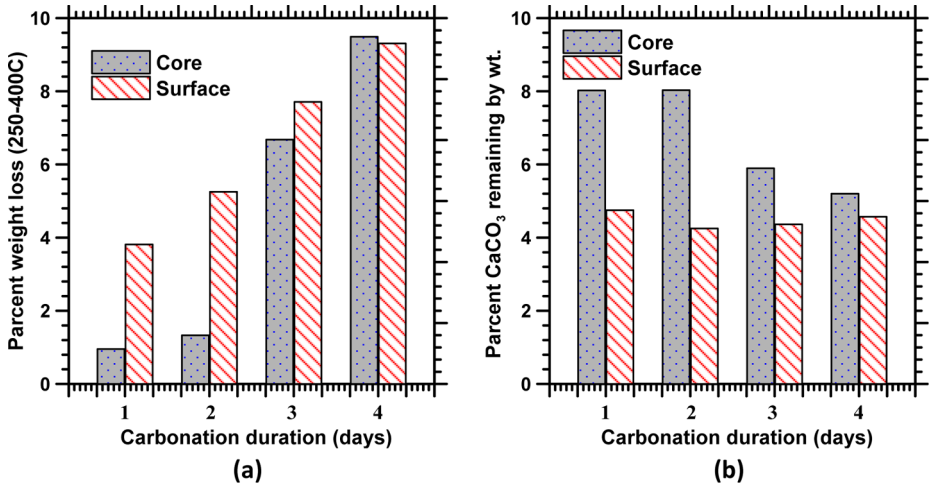

Figure 12. Effect of carbonation duration on (a) mass loss in the 250−400 °C in TGA and (b) amount of $CaCO_3$ remaining.

carbonated cylindrical specimen after 1 to 4 days of carbonation and 3 days of air-exposure. The peak at 110 °C in the DTG plot (because of evaporation of water) reduces in magnitude with increases in carbonation duration especially after 2 days of carbonation, whereas the peak at 300 °C (attributable to carbonate-oxalate cancrinite group materials[27]) increases in magnitude significantly when the carbonation period is increased. Another important phenomenon observed in Figure 11 is that the difference in final weight loss between surface and core reduces as the carbonation duration is increased. This indicates that CO_2 diffusion extends to the core with an increase in exposure duration as expected. By 4 days, there is virtually no difference in the TG and DTG signatures between the core and the surface indicating that complete carbonation can be achieved in these samples. However, it must be remembered that this is a function of specimen size, constitution, and the carbonating environment. While the TG and DTG signatures indicate similar levels of carbonation in the

dx.doi.org/10.1021/am5011145 | ACS Appl. Mater. Interfaces 2014, 6, 8295−8304

core and surface of these samples, the iron particles are not completely converted into iron carbonates (not entirely desirable also, because some unreacted iron particles can be beneficial in mechanical properties) because, as the reaction products form around these particles and the moisture content in the specimens drop, the ionic diffusion coefficient decreases and the reaction becomes extremely slow.

A further analysis of the carbonation duration-dependent mass loss patterns is attempted in Figure 12. Figure 12a shows the percent mass loss in the 250−400 °C range (corresponding to the carbonate complex) and tracks the relative degree of carbonation in the surface and core of the samples. The carbonation degree is shown to increase with carbonation duration, with a significant increase in reaction product formation in the specimen core between 2 and 3 days of CO_2 exposure. The mass loss observed in the 650−800 °C range in the DTG plots corresponds to thermal decomposition of calcium carbonate (from the added limestone) into calcium oxide. The amount of calcium carbonate remaining in the system was calculated based on the stoichiometry of the thermal decomposition reaction of calcium carbonate. The percentage of unreacted calcium carbonate present in the system for various carbonation durations is shown in Figure 12b which shows a significant difference in the amount of unreacted $CaCO_3$ between the core and the surface in the first 2 days of carbonation. However, this difference is reduced as the carbonation period is increased to 3 to 4 days. The amount of unreacted $CaCO_3$ is generally the same at the specimen surface at all carbonation durations as can be observed from Figure 12b. As carbonation proceeds, the amount of $CaCO_3$ remaining in the core drops because of the consumption of some limestone in the reaction product formation. Between 2 and 3 days, there is a reduction in the amount of calcium carbonates present in the core, which corresponds to the increase in the amount of carbonate complex shown in Figure 12a. Thus, it can be inferred that some portion of calcium carbonate is utilized to form the carbonate-oxalate complex and the remaining unreacted limestone is decomposed in that temperature range. Since, the thermal analysis study confirms similar degree of carbonation of core and surface after 4 days of carbonation, restricting the upper limit of carbonation duration to 4 days in the studies reported here is justified.

4. CONCLUSIONS

This Research Article has reported experimental results and analysis on the effect of source materials and curing conditions on mechanical properties of a unique binder system that utilizes the carbonation of metallic iron powder for cementation properties. The experiments carried out here showed that waste iron powder in combination with commonly used concrete ingredients, such as fly ash, limestone powder, and metakaolin as minor components can be carbonated to produce a binding material with acceptable properties for a wide range of construction applications. In addition, this route of binder formation is a method of CO_2 minimization both in terms of CO_2 trapping in the form of carbonate formation, as well as provision of an alternate structural binder that helps reduce portland cement consumption. Compressive strengths in the 30−35 MPa range were obtained after 4 days of carbonation.

The compressive strength of the binder systems were significantly influenced by the fly ash content. While limestone in the chosen range did not influence the strength at lower fly ash contents, the synergistic effects were evident at higher fly ash contents. Metakaolin primarily influenced the processing of the binder by providing cohesion to the mixtures. CO_2 exposure duration and air curing duration were also found to be influential on the mechanical properties of the binder. The effect of air-exposure time on compressive strength was found to be negligible at lower levels of carbonation (1−2 days) although the sensitivity increased significantly at higher carbonation durations (3−4 days). Thermogravimetric analysis showed that the carbonation efficiency of iron carbonate binders is very sensitive to the overall starting material composition. The difference in mass loss between surface and core reduced significantly as the CO_2 diffusion is extended to the core with an increase in carbonation duration. The distinct DTG peak at 300 °C which is very common for carbonate−oxalate cancrinite group materials was evident in the signals of these binders. The mass loss in the temperature range of 250−400 °C increased as the carbonation duration increased, indicating the formation of more carbonate-bearing binding products. $CaCO_3$ content in the specimen core decreased when the carbonation was increased, which served as an indication of the consumption of limestone in reaction product formation. These results point to the fact that the reaction product formation increases as the carbonation progresses resulting in a denser structure and therefore better mechanical performance.

■ ASSOCIATED CONTENT

Ⓢ Supporting Information

Chemical composition of the iron powder, fly ash, metakaolin, and ordinary portland cement are provided, the Harvard miniature compaction apparatus and the ejector, along with the cylindrical specimens prepared for compressive strength tests, field-applicable methodology to supply CO_2 to an iron-based binder concrete in the field to enable reactions to proceed for longer durations and develop adequate properties. This material is available free of charge via the Internet at http://pubs.acs.org.

■ AUTHOR INFORMATION

Corresponding Author

*E-mail: Narayanan.Neithalath@asu.edu.

Notes

The contents of this paper reflect the views of the authors who are responsible for the facts and accuracy of the data presented herein and do not necessarily reflect the views and policies of NSF nor do the contents constitute a standard, specification, or a regulation.

The authors declare no competing financial interest.

■ ACKNOWLEDGMENTS

The authors sincerely acknowledge the support from National Science Foundation (CMMI 1353170) towards the conduct of this study. This study was carried out in the Laboratory for the Science of Sustainable Infrastructural Materials (LS-SIM), and the support that has made this laboratory possible is acknowledged. Raw materials were provided by Schuff Steel, Iron Shell LLC, Omya AG, Headwaters Inc., and Burgess Pigments, which are acknowledged.

■ REFERENCES

(1) Bachu, S.; Gunter, W. D.; Perkins, E. H. Aquifer Disposal of CO_2: Hydrodynamic and Mineral Trapping. *Energy Convers. Manage.* **1994**, *35*, 269−279.

(2) Holloway, S. An Overview of the Underground Disposal of Carbon Dioxide. *Energy Convers. Manage.* **1997**, *38*, S193−S198.
(3) Kaszuba, J. P.; Janecky, D. R.; Snow, M. G. Carbon Dioxide Reaction Processes in a Model Brine Aquifer at 200 °C and 200 bar: Implications for Geologic Sequestration of Carbon. *Appl. Geochem.* **2003**, *18*, 1065−1080.
(4) Xu, T. F.; Apps, J. A.; Pruess, K. Numerical Simulation of CO_2 Disposal by Mineral Trapping in Deep Aquifers. *Appl. Geochem.* **2004**, *19*, 917−936.
(5) Flaathen, T. K.; Gislason, S. R.; Oelkers, E. H.; Sveinbjörnsdóttir, A. E. Chemical Evolution of the Mt. Hekla, Iceland, Groundwaters: A Natural Analogue for CO_2 Sequestration in Basaltic Rocks. *Appl. Geochem.* **2009**, *24*, 463−474.
(6) Gislason, S. R.; Wolff-Boenisch, D.; Stefansson, A.; Oelkers, E. H.; Gunnlaugsson, E.; Sigurdardottir, H.; Sigfusson, B.; Broecker, W. S.; Matter, J. M.; Stute, M.; Axelsson, G.; Fridriksson, T. Mineral Sequestration of Carbon Dioxide in Basalt: A Pre-injection Overview of the CarbFix Project. *Int. J. Greenhouse Gas Control* **2010**, *4*, 537−545.
(7) Qafoku, O.; Kovarik, L.; Kukkadapu, R. K.; Ilton, E. S.; Arey, B. W.; Tucek, J.; Felmy, A. R. Fayalite Dissolution and Siderite Formation in Water-Saturated Supercritical CO_2. *Chem. Geol.* **2012**, *332*−*333*, 124−135.
(8) Klein, E.; Lucia, M. D.; Kempka, T.; Kühn, M. Evaluation of Long-term Mineral Trapping at the Ketzin Pilot Site for CO_2 Storage: An Integrative Approach Using Geochemical Modeling and Reservoir Simulation. *Int. J. Greenhouse Gas Control* **2013**, *19*, 720−730.
(9) Xu, T.; Apps, J. A.; Pruess, K.; Yamamoto, H. Numerical Modeling of Injection and Mineral Trapping of CO_2 with H_2S and SO_2 in a Sandstone Formation. *Chem. Geol.* **2007**, *242*, 319−346.
(10) Naganuma, T.; Yukimura, K.; Todaka, N.; Ajima, S. Concept and Experimental Study for a New Enhanced Mineral Trapping System by Means of Microbially Mediated Processes. *Energy Proc.* **2011**, *4*, 5079−5084.
(11) Hobbs, D. W. The Tensile Strength of Rocks. *Int. J. Rock Mech. Miner. Sci.* **1963**, *I*, 385−396.
(12) Hobbs, D. W. Rock Tensile Strength and Its Relationship to Number of Alternative Measures of Rock Strength. *Int. J. Rock Mech. Miner. Sci.* **1967**, *4*, 115−127.
(13) Herget, G.; Unrug, K. In Situ Rock Strength from Triaxial Testing. *Int. J. Rock Mech. Min, Sci.* **1976**, *13*, 299−302.
(14) Park, A. A.; Jadhav, R.; Fan, L. CO_2 Mineral Sequestration: Chemically Enhanced Aqueous Carbonation of Serpentine. *Can. J. Chem. Eng.* **2003**, *81*, 885−890.
(15) Matter, J. M.; Kelemen, P. B. Permanent Storage of Carbon Dioxide in Geological Reservoirs by Mineral Carbonation. *Nat. Geosci.* **2009**, *2*, 837−841.
(16) Xu, T.; Apps, J. A.; Pruess, K. Mineral Sequestration of Carbon Dioxide in a Sandstone−Shale System. *Chem. Geol.* **2005**, *217*, 295−318.
(17) Rivera-Grau, L. M.; Casales, M.; Regla, I.; Ortega-Toledo, D. M.; Gonzalez-Rodriguez, J. G.; Martinez, G. L. CO_2 Corrosion Inhibition by Imidazoline Derivatives Based on Coconut Oil. *Int. J. Electrochem. Sci.* **2012**, *7*, 13044−13057.
(18) Wu, S. L.; Cui, Z. D.; He, F.; Bai, Z. Q.; Zhu, S. L.; Yang, X. J. Characterization of the Surface Film Formed from Carbon Dioxide Corrosion on N80 Steel. *Mater. Lett.* **2004**, *58*, 1076−1081.
(19) Nordsveen, M.; Nešić, S.; Nyborg, R.; Stangeland, A. A Mechanistic Model for Carbon Dioxide Corrosion of Mild Steel in the Presence of Protective Iron Carbonate Films—Part 1: Theory and Verification. *Corros. Sci.* **2003**, *59*, 443−456.
(20) Nesic, S.; Postlethwaite, J.; Olsen, S. An Electrochemical Model for Prediction of Corrosion of Mild Steel in Aqueous Carbon Dioxide Solutions. *Corros. Sci.* **1996**, *52*, 280−294.
(21) Sun, J. B.; Zhang, G. A.; Liu, W.; Lu, M. X. The Formation Mechanism of Corrosion Scale and Electrochemical Characteristic of Low Alloy Steel in Carbon Dioxide-saturated Solution. *Corros. Sci.* **2012**, *57*, 131−138.
(22) Lee, S. O.; Tran, T.; Jung, B. H.; Kim, S. J.; Kim, M. J. Dissolution of Iron Oxide Using Oxalic Acid. *Hydrometallurgy* **2007**, *87*, 91−99.
(23) Taxiarchou, M.; Panias, D.; Douni, I.; Paspaliaris, I.; Kontopoulos, A. Removal of Iron from Silica Sand by Leaching with Oxalic Acid. *Hydrometallurgy* **1997**, *46*, 215−227.
(24) Ambikadevi, V. R.; Lalithambika, M. Effect of Organic Acids on Ferric Iron Removal from Iron-Stained Kaolinite. *Appl. Clay Sci.* **2000**, *16*, 133−145.
(25) Faire, A. G.; Remolar, D. F.; Dohm, J. M.; Baker, V. R.; Amils, R. Inhibition of Carbonate Synthesis in Acidic Oceans on Early Mars. *Nature* **2004**, *431*, 423−426.
(26) Kumar, R.; Thangaraj, A.; Bhat, R. N.; Ratnasamy, P. Synthesis of Iron-Silicate Analogs of Zeolite Beta. *Zeolites* **1990**, *10*, 85−89.
(27) Olysych, L. V.; Vigasina, M. F.; Melchakova, L. V.; Ogorodova, L. P.; Pekov, I. V.; Chukanov, N. V. Thermal Evolution and Thermochemistry of the Cancrinite Group Carbonate−Oxalate Mineral. *Geochem. Int.* **2011**, *49*, 731−737.
(28) Moon, H. Y.; Kim, H. S.; Choi, D. S. Relationship between Average Pore Diameter and Chloride Diffusivity in Various Concretes. *Constr. Build. Mater.* **2006**, *20*, 725−732.
(29) Ghafari, E.; Costa, H.; Julio, H.; Portugal, A.; Duraes, L. The Effect of Nanosilica Addition on Flowability, Strength and Transport Properties of Ultra High Performance Concrete. *Mater. Des.* **2014**, *59*, 1−9.
(30) Fajardo, V. M. S.; Torres, M. E.; Moreno, A. J. Study of the Pore Structure of the Lightweight Concrete Block with Lapilli as an Aggregate to Predict the Liquid Permeability by Dielectric Spectroscopy. *Constr. Build. Mater.* **2014**, *53*, 225−234.
(31) Elrahman, M. A.; Hillemeier, B. Combined Effect of Fine Fly Ash and Packing Density on the Properties of High Performance Concrete: An Experimental Approach. *Constr. Build. Mater.* **2014**, *58*, 225−233.